Epitaxial graphene on cubic SiC(111)/Si(111) substrate

A. Ouerghi,[1,a] A. Kahouli,[1] D. Lucot,[1] M. Portail,[2] L. Travers,[1] J. Gierak,[1] J. Penuelas,[3]
P. Jegou,[4] A. Shukla,[5] T. Chassagne,[6] and M. Zielinski[6]

[1]*CNRS-Laboratoire de Photonique et de Nanostructures (LPN), Route de Nozay, 91460 Marcoussis, France*
[2]*CNRS-CRHEA, Rue Bernard Gregory, 06560 Valbonne, France*
[3]*INL UMR5270-CNRS, Ecole Centrale de Lyon, 36 Avenue Guy de Collongue, 69134 Ecully, France*
[4]*DSM/IRAMIS/SCM, CEA Saclay, 91191 Gif-sur-Yvette, France*
[5]*IMPMC, CNRS-UMR7590, Université Pierre et Marie Curie-Paris 6, 140 rue de Lourmel,*
Paris F-75015, France
[6]*NOVASiC, Savoie Technolac, Arche Bat 4, BP267, 73375 Le Bourget du Lac, France*

Epitaxial graphene films grown on silicon carbide (SiC) substrate by solid state graphitization is of great interest for electronic and optoelectronic applications. In this paper, we explore the properties of epitaxial graphene films on 3C-SiC(111)/Si(111) substrate. X-ray photoelectron spectroscopy and scanning tunneling microscopy were extensively used to characterize the quality of the few-layer graphene (FLG) surface. The Raman spectroscopy studies were useful in confirming the graphitic composition and measuring the thickness of the FLG samples. © *2010 American Institute of Physics*. [doi:10.1063/1.3427406]

Due to its unique mechanical, physical, and chemical properties, graphene has generated intense experimental and theoretical activities in material science and condensed-matter physics.[1] The successful microcleaving of graphene from highly oriented pyrolytic graphite has opened up exciting possibilities for wide spectra of experimental investigations.[2] Indeed high carrier mobility and ballistic transport at room temperature,[3] quantum confinement in nanoscale ribbons,[4] and single-molecule gas detection sensitivity qualify graphene as a promising material for many applications such as microelectronics, sensing, or catalysis.[5] However, reliable and economically viable methods for producing large-area of single-crystalline graphene domains with uniform thickness are still needed. Up to now various methods have been explored including deposition of graphene oxide films from a liquid suspension followed by chemical reduction,[6] chemical vapor deposition on transition metals,[7,8] and ultrahigh vacuum (UHV) annealing of SiC.[9] Finally if the use of single crystal hexagonal SiC substrates has been demonstrated to be one of the more reliable ways to provide high quality graphene films,[9] commercial bulk SiC substrates remain limited in size and expensive. These could be seen as a major risk for the development of graphene based devices. In order to address this issue, the *heteroepitaxy* of cubic polytype (3C-SiC) on larger diameter (6 in.) silicon wafers was proposed.[10] But high-quality growth of 3C-SiC epilayers remains delicate, especially concerning the (111) oriented films that experience high residual stress, generating an important bowing and possible film cracking.[11] Many efforts were carried out to overcome these problems and get a better insight in the defect generation during the growth mechanism,[12,13] making 3C-SiC(111)/Si heteroepilayers a suitable template of great interest for graphene elaboration.

In this paper, we report the growth of graphene on 3C-SiC(111). Growth, structure, and electronic properties of the films were investigated in details using scanning tunneling

microscopy (STM) and x-ray photoelectron spectroscopy (XPS). Additional informations were obtained from low-energy electron diffraction (LEED) and micro-Raman spectroscopy.

Graphene on Si-terminated 3C-SiC(111)/Si(111) substrates were prepared in UHV by electron-bombardment heating [Fig. 1(a)]. Substrates were first degassed for several hours at 600 °C under UHV conditions and then annealed under a low (0.1 nm/min) Si flux at 900 °C to remove the native oxide. The base pressure of the system was maintained around 2×10^{-10} Torr with a maximum peak pressure of 10^{-9} Torr during the graphitization process. Immediately after this, the samples were cooled down to room temperature and transferred *ex situ* from the growth chamber to the RT-STM and then to a XPS experiment. For further characterization the samples were again degassed at 600 °C for 30 min. XPS experiments were carried out on a Kratos analytical system using $Al_{K\alpha}$ monochromatized source with an energy resolution of ~350 meV. Raman spectroscopy was performed at room temperature with a T64000 spectrometer. A frequency doubled NdYVO4 laser with a wavelength of
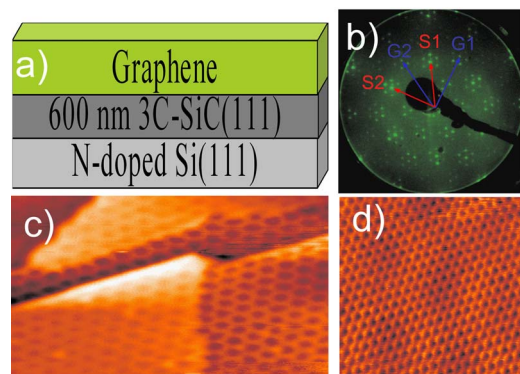

FIG. 1. (Color online) (a) Schematic diagram of graphene as used in our investigations. (b) LEED pattern at 114 eV showing the diffraction spots due to the SiC(111) substrate (S1, S2) and the graphene lattice (G1, G2). (c) STM images (27×15 nm^2) of the surface of graphene/3C-SiC(111). (d) Honeycomb type structures (5×5 nm^2) (-45 mV, 0.2 nA).

[a]Electronic mail: ouerghi@lpn.cnrs.fr.

514 nm was used for excitation and a confocal optical microscope was employed to record micro-Raman spectra with a spatial resolution of 1 μm.

Long range order modifications experienced by the surface after thermal annealing were investigated by LEED measurements. Initially, (3×3) and $(\sqrt{3} \times \sqrt{3})R30°$ diffraction patterns were observed by annealing the sample in a flux of Si at 900 °C and 1050 °C, respectively. These diffraction patterns were attributed to a Si rich surface.[14] Between 1100 and 1200 °C, a $(6\sqrt{3} \times 6\sqrt{3})R30°$ begins to develop. Figure 1(b) shows the LEED pattern of the sample after graphitization at 1250 °C. Two contributions can be clearly distinguished in the LEED diagram. The first one arising from the (1×1) graphene layer confirms the presence of this material at the surface of the sample. The second one which is characterized by isotropic (circular) 1/6 fractional spots is the $(6\sqrt{3} \times 6\sqrt{3})R30°$ reconstruction. This structure can be represented as a precursor phase of graphitization, i.e., a carbon layer not exhibiting the usual properties of graphene.[14] It must be outlined here that the successive surface reconstructions steps observed during the thermal treatment of the 3C-SiC(111)/Si(111) are totally similar to those observed on Si terminated 6H or 4H-SiC(0001) substrates.[14] STM image of this surface at higher bias (-2 V) shows two-dimensional hexagonal structures patterns in real space with a periodicity of 18 Å are observed in both directions [Fig. 1(c)], which is consistent to the (6×6) surface reconstruction with respect to the unreconstructed 3C-SiC(111) surface. This structure is attributed to a C-rich $(6\sqrt{3} \times 6\sqrt{3})R30°$ reconstruction of the SiC precursor layer below the graphene. It has been interpreted as a multiple diffraction between an unreconstructed SiC substrate and the graphite overlayer rotated by 30° with respect to the substrate.[15,16] Then, at lower bias sample at -45 meV, a honeycomb lattice can be put in evidence [Fig. 1(d)], superposed on the $(6\sqrt{3} \times 6\sqrt{3})R30°$ structure. The periodicity of this structure is equal to 2.5 ± 0.1 Å which is in good agreement with the (1×1) graphene lattice.[16] Similar images have been observed in STM studies of single-layer graphene, where both sublattices (A-B) are imaged at almost the same intensity.[15] This asymmetry in the surface electronic environment results in a threefold symmetry ("six-for-three") pattern in which three bright or dark features can be observed for each set of six carbon atoms.

Chemical states of thin graphene layers were also probed using the XPS technique. XPS spectra were recorded on C 1s core level in dependence on the temperature annealing, in order to track the chemical environment variations experienced by the sample after each thermal annealing [Fig. 2(a)]. The C 1s peak at 284.8 eV associated with graphene appears clearly at 1200 °C, for higher temperature and longer annealing time, graphene peak intensity continues to increase. The assumption of an epitaxial graphene layer is supported by the following observations: (i) The pronounced asymmetrical shape of the peak confirms the conductive state of carbon,[14,17] (ii) The hight energy of C 1s peak shift from 285.2 to 284.5 eV which confirms the presence of sp^2 hybridized C–C bonds as the temperature increases, (iii) The attenuation of the SiC component. Applying a curve-fit procedure to the C 1s spectra of a graphene sheet grown on SiC(111) at 1250 °C, we obtained three components located at binding energies of 283.6, 284.7, and 285.2 eV. These components correspond, to bulk SiC, graphene, interface
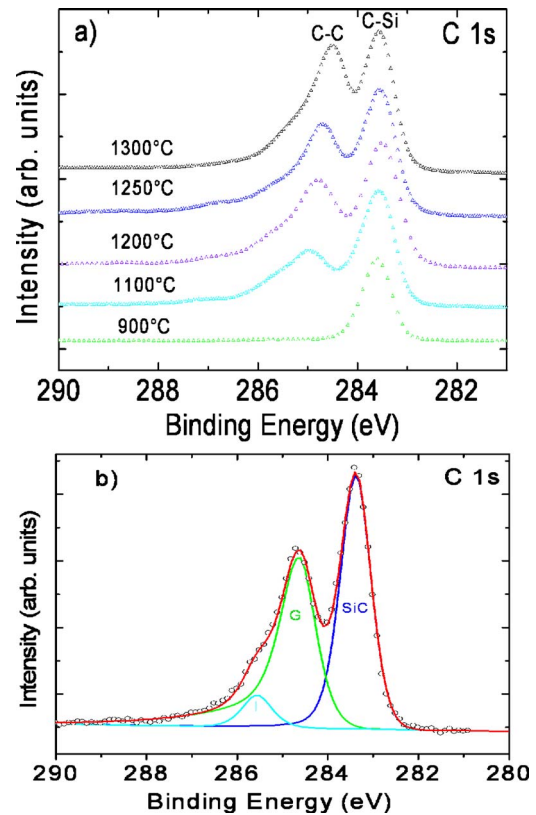

FIG. 2. (Color online) (a) C 1s XPS spectra of the fully grown graphene on 3C-SiC(111) for different temperatures. (b) XPS spectra of the C 1s core level for graphene with a Doniach–Sunjic lineshape analysis (red line); Decomposition with bulk and two surfaces components identified by B, G, and I, respectively.

$[(6\sqrt{3} \times 6\sqrt{3})R30°]$ layers, and are denoted as bulk SiC, G (still asymmetrically), and I, respectively [Fig. 2(b)]. Indeed this peak (I) is associated with an interfacial layer between the graphene and the SiC(111) substrate without strong rearrangement of the surface structure and is accompanied by the formation of chemical bonds between the substrate and graphene layer.[17] We were able to determine the graphene film thicknesses by measuring the attenuation of the C 1s peak associated with the SiC substrate at 283.6 eV. For the sample annealed at 1250 °C during 10 min a graphene film of approximately 2 monolayer (ML) thick is formed and the surface contribution (I) corresponding to less than 0.6 ML.[14,17] This thickness measurement is corroborated by the attenuation observed in the Si 2p XPS.

Further details on the electronic properties of the graphene film were acquired using micro-Raman spectroscopy. Figure 3 shows Raman spectra of $(6\sqrt{3} \times 6\sqrt{3})R30°$ reconstruction and two-layer graphene grown on Si-terminated 3C-SiC(111). Raman spectrum of $(6\sqrt{3} \times 6\sqrt{3})R30°$ (annealing at 1150 °C for 10 min) shows the dominant band of the $(6\sqrt{3} \times 6\sqrt{3})R30°/3C-SiC(111)$ which may be attributed to transverse optical (TO) phonon modes at 1510 cm^{-1}.[18] For the sample annealed at 1250 °C during 10 min, three additional bands appears at around 1350, 1596, and 2700 cm^{-1}, which are attributed, respectively, to the D, G, and 2D bands. The presence of a single G and 2D bands indicates that our graphene, consists of a few-layer graphene (FLG). The appearance of the D bands at 1350 cm^{-1} is attributed to the defects or structural disorder. The defects including vacancies and distortions may be attributed to twist-
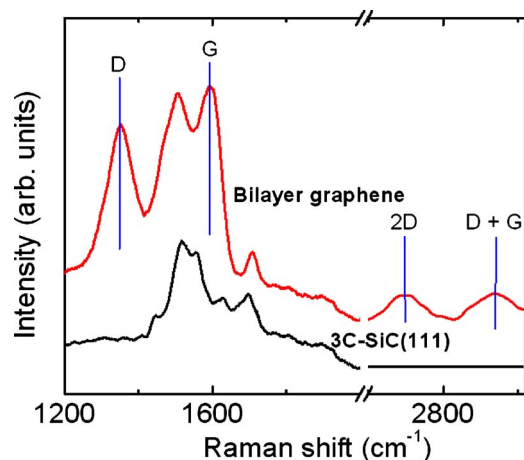
FIG. 3. (Color online) Micro-Raman characterization of graphene/3C-SiC(111): Comparison of Raman spectra at $(6\sqrt{3} \times 6\sqrt{3})$ interface layer/3C-SiC(111) (black) and bilayer graphene/3C-SiC(111) (red).

ing, corrugation, and steps edges.[18] It should be also noted that the samples with a $(6\sqrt{3} \times 6\sqrt{3})R30°$ reconstructed surface show no detectable Raman intensity at 1570 cm^{-1}. This confirms that the interfacial (I component) carbon layer/buffer layer is covalently bonded to the substrate. In addition to that it is not responsible for electronic properties and the second C rich plane which constitutes the first graphene layer.[19] Moreover, significant blueshifts of G-band (16 cm^{-1}) and 2D-band ($\sim$25 cm^{-1}) of epitaxial graphene layer are observed compared to those of graphene made by micromechanical cleavage. A possible cause for this blueshift may be compressive strain which builds up during the cool down procedure or charge doping from the substrate. The influence of the charge has been studied by Das *et al.*[20] They observe an upshift of the *G*-peak frequency by as much as 20 cm^{-1} when the graphene layer is doped with electrons with a density of 4×10^{13} cm^{-2}. It is shown that the dependence of doping on shift in the 2D-band is very weak. It is roughly 10%–30% compared to that of G-band (3 and 5 cm^{-1}).[20] Therefore, the 25 cm^{-1} 2D-band shift is too large to be achieved by electron/hole dopings. We attribute it to the interaction of SiC(111) substrate with epitaxial graphene, most probably the strain effect, whereby the strain changes the lattice constant of graphene, hence the Raman peak frequencies. Assuming that the mismatch between the graphene and the $(6\sqrt{3} \times 6\sqrt{3})R30°$ reconstructed surface of 3C-SiC(111) is completely relaxed at the growth temperature. A residual *compressive* strain arises during sample cooling to room temperature because of the large difference in the coefficients of linear thermal expansion between graphene and SiC. The strain in our graphene has been deduced at RT from the Raman shift of the 2D bands (25 cm^{-1}). It is close to 0.7%, which is in good agreement with the previously reported results of epitaxial graphene on 6H-SiC(0001) substrates.[18,21]

We have successfully demonstrated a new technique for the synthesis of FLG on Si-terminated 3C-SiC(111)/Si(111) substrates. The growth of FLG was confirmed by LEED and STM. XPS and Raman Spectroscopy were both found to provide accurate estimation of the graphene layer thickness. The 16 cm^{-1} higher frequency shift of the G peak relative to micromechanically cleaved graphene on SiO$_2$ was associated with a charge exchange phenomena resulting form the underlying 3C-SiC(111) substrate and compressive strain of graphene. The much greater (25 cm^{-1}) blueshift observed for the 2D-band may be correlated with compressive strain. The proposed low cost and scalable approach may be of considerable interest for future industrial applications of graphene films based devices.

[1] K. S. Novoselov, A. K. Geim, S. V. Morozov, D. Jiang, M. I. Katsnelson, I. V. Grigorieva, S. V. Dubonos, and A. A. Firsov, Nature (London) **438**, 197 (2005).
[2] Y. B. Zhang, Y. W. Tan, H. L. Stormer, and P. Kim, Nature (London) **438**, 201 (2005).
[3] K. S. Novoselov, A. K. Geim, S. V. Morozov, D. Jiang, Y. Zhang, S. V. Dubonos, I. V. Grigorieva, and A. A. Firsov, Science **306**, 666 (2004).
[4] B. Özyilmaz, P. Jarillo-Herrero, D. Efetov, and P. Kim, Appl. Phys. Lett. **91**, 192107 (2007).
[5] F. Schedin, A. K. Geim, S. V. Morozov, E. W. Hill, P. Blake, M. I. Katsnelson, and K. S. Novoselov, Nat. Mater. **6**, 652 (2007).
[6] G. Eda, G. Fanchini, and M. Chhowalla, Nat. Nanotechnol. **3**, 270 (2008).
[7] K. S. Kim, Y. Zhao, H. Jang, S. Y. Lee, J. M. Kim, K. S. Kim, J. H. Ahn, P. Kim, J. Y. Choi, and B. H. Hong, Nature **457**, 706 (2009).
[8] A. Reina, X. Jia, J. Ho, D. Nezich, H. Son, V. Bulovic, M. S. Dresselhaus, and J. Kong, Nano Lett. **9**, 30 (2009).
[9] C. Berger, Z. M. Song, X. B. Li, X. S. Wu, N. Brown, C. Naud, D. Mayo, T. B. Li, J. Hass, A. N. Marchenkov, E. H. Conrad, P. N. First, and W. A. de Heer, Science **312**, 1191 (2006).
[10] A. Severino, C. Bongiorno, N. Piluso, M. Italia, M. Camarda, M. Mauceri, G. Condorelli, G. M. A. di Stefano, B. Cafra, A. La Magna, and F. La Via, Thin Solid Films **518**(6), S165 (2010).
[11] S. Nishino, H. Suhara, H. Ono, and H. Matsunami, J. Appl. Phys. **61**, 4889 (1987).
[12] S. Roy, M. Portail, T. Chassagne, J. M. Chauveau, P. Vennéguès, and M. Zielinski, Appl. Phys. Lett. **95**, 081903 (2009).
[13] M. Portail, M. Zielinski, T. Chassagne, S. Roy, and M. Nemoz, J. Appl. Phys. **105**, 083505 (2009).
[14] K. V. Emtsev, F. Speck, Th. Seyller, L. Ley, and J. D. Riley, Phys. Rev. B **77**, 155303 (2008).
[15] P. Lauffer, K. V. Emtsev, R. Graupner, Th. Seyller, L. Ley, S. A. Reshanov, and H. B. Weber, Phys. Rev. B **77**, 155426 (2008).
[16] P. Mallet, F. Varchon, C. Naud, L. Magaud, C. Berger, and J. Y. Veuillen, Phys. Rev. B **76**, 041403 (2007).
[17] J. Penuelas, A. Ouerghi, D. Lucot, C. David, J. Gierak, H. Estrade-Szwarckopf, and C. Andreazza-Vignolle, Phys. Rev. B **79**, 033408 (2009).
[18] Z. H. Ni, W. Chen, X. F. Fan, J. L. Kuo, T. Yu, A. T. S. Wee, and Z. X. Shen, Phys. Rev. B **77**, 115416 (2008).
[19] F. Varchon, R. Feng, J. Hass, X. Li, B. N. Nguyen, C. Naud, P. Mallet, J.-Y. Veuillen, C. Berger, E. H. Conrad, and L. Magaud, Phys. Rev. Lett. **99**, 126805 (2007).
[20] A. Das, S. Pisana, B. Chakraborty, S. Piscanec, S. K. Saha, U. V. Waghmare, K. S. Novoselov, H. R. Krishnamurthy, A. K. Geim, A. C. Ferrari, and A. K. Sood, Nat. Nanotechnol. **3**, 210 (2008).
[21] N. Ferralis, R. Maboudian, and C. Carraro, Phys. Rev. Lett. **101**, 156801 (2008).